JOM
DOI: 10.1007/s11837-017-2506-4

Production and Characterization of TiO_2 Nanofilms for Hemocompatible and Photocatalytic Applications

C.E. SCHVEZOV,[1,2,3] M.L. VERA,[1] J.M. SCHUSTER,[1] and M.R. ROSENBERGER[1]

1.—Instituto de Materiales de Misiones (IMAM), CONICET – UNaM, Félix de Azara 1552, 3300 Posadas, Misiones, Argentina. 2.—e-mail: schvezov@fceqyn.unam.edu.ar. 3.—e-mail: schvezov@gmail.com

Titanium dioxide (TiO_2) coatings are currently produced for hemocompatible and photocatalytic applications by using two techniques: sol–gel and anodic oxidation. In this review, the research advances on TiO_2 nanofilms produced with these techniques are presented, with a focus on different aspects such as process parameters, morphology, roughness, crystal structure, adhesion, wear and erosion resistance, corrosion resistance, hemocompatibility, toxicity, plaque and bacterial adhesion, and heterogeneous photocatalysis of immobilized porous material. This review was presented at the 3rd Pan American Materials Congress at the 2017 TMS Annual Meeting and Exhibition in San Diego, California, USA.

INTRODUCTION

In recent years, there has been an increasing interest in studying the properties of titanium dioxide (TiO_2), a semiconductor that has shown potential uses in many applications. Besides its traditional use, which is based on its high reflectivity, TiO_2 is currently being used in many fields, ranging from energy to environmental and biomedical. Because each type of application has specific requirements, the production process and properties of the coating should be in accordance with its specific use. In the energy field, the potential use of a gel containing nanostructured TiO_2 as anode material for lithium ion batteries has been recently reviewed.[1,2] In environmental applications, TiO_2 is a well-known photocatalyst used for water disinfection and decontamination when irradiated under UV light.[3] Although this technology uses TiO_2 suspensions, which require expensive and time-consuming separation processes, the overall process may be optimized by immobilization of TiO_2 on suitable substrates.[4] In biomedical applications, TiO_2 is used as a coating of titanium alloys in dental implants because of its osseointegration properties,[5–7] and it can be potentially used in devices like stents and heart valves as a result of its high hemocompatibility.[8–13]

Regarding its structure, TiO_2 may either be in an amorphous form or crystalize as three different structures: (1) as rutile, which is the stable form normally found in nature; (2) as anatase, which has a tetragonal crystal structure but different structural parameters; and (3) as brookite, which is an unstable form, with an orthorhombic structure. Producing the right crystal structure or mixture of structures becomes important to obtain the optimal desired properties of the coating. Among others, TiO_2 presents properties as a semiconductor, which is important to define its hemocompatible and photocatalytic properties. In addition, the desired surface of the coating differs drastically depending on the application (Fig. 1). For hemocompatible applications, the surface must be as smooth as possible, whereas for photocatalytic applications, the surface should be rough and porous, with the largest possible ratio of contact surface area versus mass or volume of material. Therefore, a perfectly smooth rutile coating is ideal for hemocompatible applications, whereas a rough anatase coating is ideal for photocatalytic applications. In addition, hemocompatible coatings should comply with specific requirements associated with their contact with blood, and if the coating is a moving part, mechanical requirements must be achieved as well. Besides their hemocompatibility, hemocompatible coatings must not promote plaque or bacteria adhesion, must be nontoxic, and

Published online: 10 August 2017

must have good corrosion properties. In photocatalytic devices, the coating must have catalytic performance and good adhesion and must be resistant to abrasion and erosion.

Considering that, as mentioned, TiO_2 coatings should satisfy specific requirements, the production processes will strongly depend on their use. For instance, in the case of hemocompatible and photocatalytic coatings on titanium substrates, the production processes that can be used are chemical vapor deposition, physical vapor deposition, electrodeposition, electrophoresis, plasma deposition, sputtering, particle deposition, thermal oxidation, sol–gel dip/spin coating, and anodic oxidation.

Only the last two processes mentioned are reviewed in this article, and the properties of TiO_2 coatings on titanium alloys used for both medical applications (as hemocompatible material with potential use in heart valve construction) and photocatalytic applications are presented.

PRODUCTION PROCESSES

Sol–Gel Dip Coating

The sol–gel process is a chemical synthesis of a colloidal suspension of Ti compounds surrounded by ligands that polymerize during the sol aging process, forming a gel.[14] Then, the sample is dip-coated by immersion and withdrawal from the sol. The main advantages of this technique are that it requires simple equipment, can be done at room temperature, there are no limitations on the nature of the substrate, and it is possible to make in situ doping of the coating.[14] The most important parameter during the process is the extraction velocity, which defines the thickness of the coating. The coatings obtained by means of this technique are amorphous and a heat treatment is necessary to produce partial crystalline coatings.[12,15]

This technique has been used to produce coatings by using titanium tetrabutoxide (TiBu), isopropanol (ISP), water (H_2O), hydrochloric acid (HCl) and ethyl acetoacetate (EAA), and two suspensions with the following molar proportions H_2O/EAA/ISP/HCl/TiBu: 1/0.5/20/51.3/1 and 3.5/1/20/51.3/1.[16] The former had a gel formation time of 7 months, whereas the latter had a gel formation time of 12 days. The coatings obtained were evaluated for surface finishing of the Ti-6Al-4V (TiG5) substrate, heat treatment temperatures (200°C, 500°C, 600°C, and 650°C), withdrawing velocities (1 cm/min, 2 cm/min, and 3 cm/min), aging times of the sol, and multilayers (1, 2, and 3 layers). A total number of 100 samples were produced, and their mechanical and hemocompatible properties were tested.[16] The coatings obtained had different interference color, a feature strongly correlated with the thickness determined by x-ray reflectometry.[17] The results also showed that the thickness of the coatings was directly related to the aging time of the sol and the extraction velocity. Nevertheless, the increase in thickness had a limit caused by the formation of detrimental cracks.[17]

As mentioned, a heat treatment can be applied to transform the amorphous coating into a mixed crystalline structure of anatase and rutile or, in some cases, of anatase alone. Above 650°C, the substrate oxidation is fast and marks the highest temperature limit.[16,17]

Anodic Oxidation

Coating by anodic oxidation has many advantages with respect to other methods. The process is simple, uses available chemicals, is done at ambient

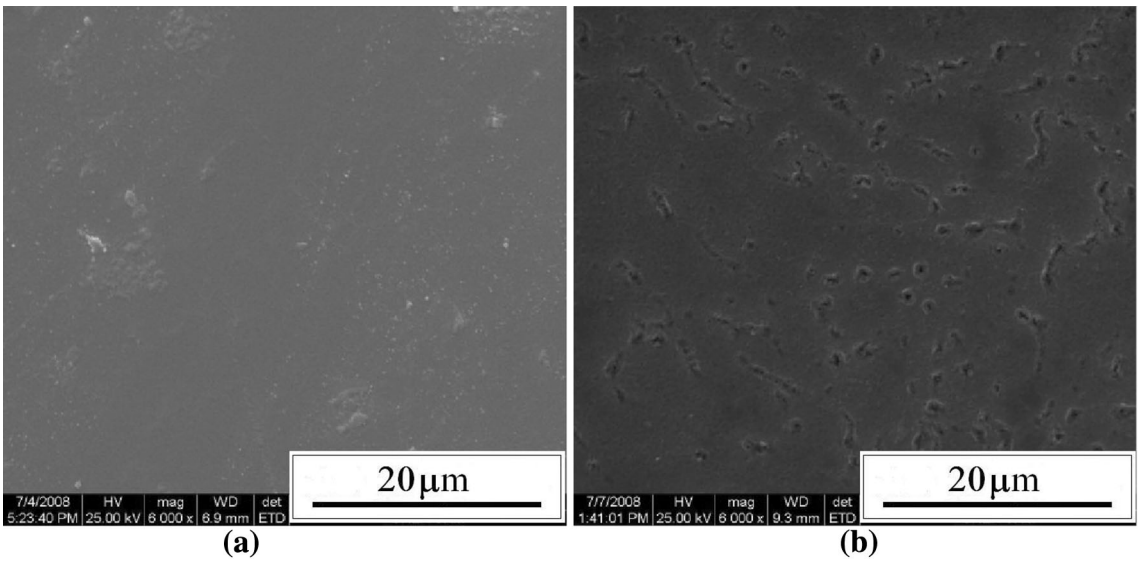

(a) (b)

Fig. 1. TiO_2 coatings obtained by anodic oxidation for (a) hemocompatible applications (smooth) and (b) photocatalytic applications (porous).

temperature, allows in situ doping by adding chemicals to the electrolyte,[18] and the coatings are stable and produced in 1 min to 5 min.[19]

The main parameters of the process are voltage, current density,[20] electrolyte concentration,[21] pH and temperature of the electrolyte,[22] and oxidation time.[23] By adjusting the values of these parameters, the structural and chemical characteristics of the coating can be modified in a wide range of values. It is possible to produce coatings with different thickness, color, morphology, and crystal structure of the oxides.[12,18,19] At low voltages or currents, the coatings obtained are amorphous, thin, homogeneous, and smooth, whereas above a certain value of voltage, the coatings are crystalline, thicker, and porous.[24–27]

Porous coatings are the result of a mechanical fracture of the film that does not stand the applied voltage and results in a dielectric breakdown,[28] which produces sparking, craters, and local fusion of the oxide.[29] The critical voltage triggering this effect depends on the type of electrolyte.

This technique has been used to produce different coatings by applying voltages from 10 V to 100 V in different acid electrolytes (sulfuric acid, phosphoric acid, and acetic acid) and different alkaline electrolytes (sodium hydroxide, potassium hydroxide, and calcium hydroxide) at concentrations from 0.025 M to 4 M.[17,30–32] The results showed that, depending on the electrolyte, at given voltages, there were two successive phenomena, breakdown and spark, which determined coating morphology, thickness, and crystalline structure. In the case of 1 M sulfuric acid solution, sparks were produced at voltages above 70 V. In the case of acetic and phosphoric acids, with lower electrical conductivity, no sparks were produced at 70 V but some breakdowns were observed. In the case of alkaline electrolytes, sparks were produced at a lower voltage of 40 V in the three cases, reducing the range to produce homogeneous coatings.[17,30–32]

Considering that hemocompatible coatings must be smooth (Ra $<$ 0.05 μm), the applied voltage must be presparking and this voltage decreases with electrolyte conductivity; sulfuric acid has been the best electrolyte and was therefore selected for this application.[30,31]

In our laboratory, we have produced coatings with thicknesses of 27 nm to 144 nm by using a 1 M solution of sulfuric acid and by applying voltages from 10 V to 60 V. X-ray reflectometry data showed a correlation of coating color versus thickness versus applied voltage, with the following relation between thickness and voltage: t [nm] = 2.41 nm/V.[17,30] In addition, we obtained partial crystallization of amorphous thin films by heat treatment for 1 h at 500°C and 600°C, which resulted in a mixture of anatase and rutile phases.[30,33] The best films for hemocompatible applications were obtained with heat treatment at 500°C.[30,33]

PROPERTIES OF THE COATINGS

Hardness and Erosion Resistance

The hardness of a material is a measure of how resistant is to indentation and defines its resistance to wear by erosion and sliding. One way of increasing the hardness of titanium alloys is by coating them with TiO_2 by either the sol–gel technique or anodic oxidation. This allows moderate-to-high increases in hardness in the range of 20% to 100% with respect to the substrate hardness, with larger increases for thicker and heat-treated coatings.[16,30]

Erosion resistance is important because in living organisms, the blood flow may reach values as high as 5 m/s and, therefore, high values of velocity gradients in the circulatory system.[34,35] The resulting shear stress may produce potential damage to a material placed in that flow, as it has been observed in mechanical heart valves.[35,36] Also, in photocatalytic reactors with recirculated flow over immobilized TiO_2 erosion may damage and inactivate the coating.

In our lab, we studied the degree of erosion of TiO_2 coatings by passing a flow from 1 m/s to 9 m/s for 11 h of a suspension 1% in weight of SiC particles, 65 μm in diameter, in a high concentration of a sucrose water solution. The flows were parallel (0°), 60°, or normal to the surface (90°).[37] The results showed that the 60° incidence produced the largest damage by erosion in a ductile type and consisted mainly of short scratches in a coma shape.[37] The quantification of the degree of wear is currently being analyzed.

Coating Adhesion

Device coatings in service must withstand applied stress by shear or compression, residual stress, and stress caused by defects or microdefects. This requirement is particularly strong in valves, stents, and other devices because, otherwise, debris or denuded surfaces may produce damage or contamination of the blood system. A widely used and accepted technique to evaluate the adhesion of coatings is the scratch test.[38–40] This technique has allowed observing at least three types of failures: cracks around the indenter, spalling off of the film, and production of a channel with total removal of the film. The analysis of these failures by different authors has shown the ductility of the film and substrate, the critical load for adhesion or cohesive failure,[41] and the intrinsic and extrinsic parameters causing the failure.[42]

In our lab, the scratch test has been used to produce several scratch lines with a spherical pivot 200 μm in radius, by applying a varying load with increasing load rates of 2 N/mm and 4 N/mm and final loads of 10 N and 20 N, respectively.[16,30,43] In the case of coatings produced by sol–gel, the results showed that thin monolayer films are more

Fig. 2. Scratches produced on two coatings oxidized in 1 M solution of sulfuric acid at 40 V and 500°C: (a) without heat treatment, load of 2 N/mm, no failure; and (b) with heat treatment at 500°C, load of 4 N/mm, failure. Load increases from left to right.

resistant than thicker films and that, in the case of thicker three-layer films, the more resistant ones are the thicker ones subjected to heat treatment at 650°C. Heat treatment with larger values of temperature and time produced stronger films. This adherence improvement resulting from a heat treatment is attributed to the formation of a stronger diffusive interface and probably to the compaction of the structure, sintering, and larger formation of a harder rutile phase, particularly in thicker films.[16] In the case of coatings produced by anodic oxidation, the films are sensitive to the ratio of the load increase. At a lower ratio of increase (2 N/mm), the coatings showed ductile behavior and did not fail up to the maximum applied load of 10 N (Fig. 2a). At the higher rate, the coatings had a more brittle behavior (Fig. 2b). Also, the critical load decreased as the temperature of the heat treatment increased. In the coatings without heat treatment, the critical load of adhesion increased with coating thickness.[30,43]

Wear Resistance

During their life in service, devices must be wear-resistant, and when placed in a living organism, the wear debris must not cause any damage by chemical or mechanical interactions with the body beyond reasonable limits.[44] The wear in coated materials, which is measured as the weight loss rate or the size of the scar produced by wear, is studied by building wear maps.[45] In thin coatings, the wear is normally studied by using reciprocanting ball-on-flat wear experiments.[16,30,46] In our lab, this method has been used to evaluate wear resistance using a spherical diamond ball 10 μm in radius oscillating at 30 Hz on the flat samples (bare or coated substrates) with an amplitude of 4 mm and loads ranging from 1 g_f to 20 g_f.[30,47,48] The wear maps obtained for the different samples tested showed that the coatings generally present a transition from mild-to-severe wear regime at a load of 5 g_f for anodic coatings and of 7 g_f for sol–gel coatings.[30,47,48] Also, crystalline coatings were more resistant than amorphous coatings, a fact explained by the higher hardness of the crystalline coatings. In all cases, in the moderate regime, the lifetime of the coating increases linearly with its thickness.[47] Typical scars are shown in Fig. 3.

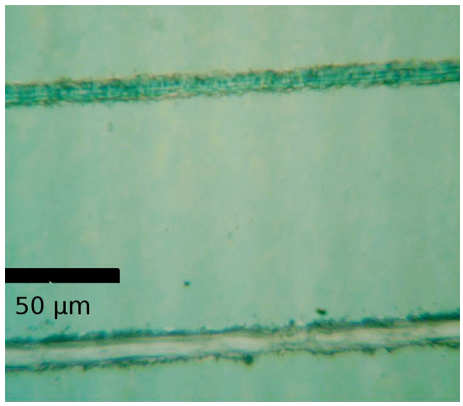

Fig. 3. Wear scars on a sol–gel coating. The upper scar (5 g_f in load) does not break the coating; the lower scar (8 g_f in load) broke the coating and exposes the substrate.

Corrosion Resistance

The by-products of a corrosion process of an oxide or metallic alloy in biological fluids continuously produce metallic ions, which may combine with biomolecules such as proteins and enzymes and may trigger allergies or toxicity effects. Therefore, evaluating the corrosion resistance of TiO_2 coatings becomes very important before using the material in devices for implants.[49] It is well known and accepted that Ti has high stability and corrosion resistance in vitro and that it accumulates in adjacent tissue, indicating some degree of corrosion in vivo.

Several solutions have been used to simulate corrosion in biological fluids.[50–54] Nevertheless, blood plasma contains chloride in a concentration strong enough to corrode metallic materials,[49] indicating that it is appropriate to study corrosion of TiO_2 solutions containing chloride by simulating blood plasma. It has also been suggested that studying corrosion in vitro by polarization curves results in an adequate method to be extrapolated to corrosion in blood plasma.[55] This technique has been used to evaluate corrosion resistance using a NaCl 0.9% solution simulating blood plasma,[12,56] and the possibility of pitting corrosion has been determined by inverted polarization.[57] The results at different voltages showed that the anodic coatings are more efficient barriers against corrosion than the natural oxide present on TiG5

substrates.[30,58] Moreover, no pitting corrosion was detected on the coated samples.[30,58] Nonetheless, the thermal treatments of the coated samples that crystallize the TiO_2 slightly deteriorated the corrosion resistance of the coatings but far from the uncoated samples.[30,58] These results and the high corrosion rate of uncoated TiG5 of 7 nm/year strongly indicate the need of coating any exposed TiG5 surface placed in a body fluid.[30,58]

Surface Free Energy and Extended Colloid Theory

The surface free energy (SFE) of solid surfaces determines the degree of interaction with the surrounding environment and defines their wettability, adsorption, and adhesion of solids, as well as the interaction of the solid surface with proteins, cells, and microorganisms present in the surrounding liquid. Therefore, it may help to explain and predict these interactions.[8,59,60]

The most practical method to determine the SFE of a solid surface is based on the measurement of the contact angle of a liquid on that surface.[61] Most methods are based on the Young equation,[60,62,63] and two of them are the geometric mean approach (GM) and the Lifshitz-van der Waals/Acid–Base (LW/AB) approach. The former considers that the total SFE (γ_i) is composed of two components: a dispersive component (γ_i^d) and a polar component (γ_i^p), such that $\gamma_i = \gamma_i^d + \gamma_i^p$, whereas the latter considers that the total SFE, or γ_i, is the result of a dispersive Lifshitz-van der Waals component (γ_i^{LW}) and contributions resulting from electron donors (γ_i^-) and electron acceptors (γ_i^+), such that the total γ_i is calculated as $\gamma_i = \gamma_i^{LW} + 2(\gamma_i^- . \gamma_i^+)^{1/2}$.[62,63]

In our lab, the water contact angle, measured for 16 samples produced with different morphologies and under different conditions, varied in a wide range of values from 60° to 90°. The calculated SFE resulted in values of the Lifshitz-van der Waals component from 30 mJ/m^2 to 42 mJ/m^2, whereas the values of the electron donor component γ_s^- ranged from 4 mJ/m^2 to 16 mJ/m^2. In all cases, the electron acceptor component γ_s^+ was negligible. When using the GM method, the values of the dispersive and polar components varied between 30 mJ/m^2 and 40 mJ/m^2 and 3 mJ/m^2 and 11 mJ/m^2, respectively.[64] The extended colloid theory (X-DLVO) can be used to explain and predict the adhesion of different bacteria, proteins, or cells in the blood to a solid surface.[65] The X-DLVO theory is based on the SFE calculated according to the LW/AB method, which includes the three components mentioned earlier (γ_i^{LW}, γ_i^- and γ_i^+) as well as a component caused by electric forces (the zeta potential), which, considering the high ionic forces in the blood, can be neglected.[65]

Adhesion can be expected when the total interaction potential (ΔG_{TOT}), which includes the LW (ΔG_{TOT}^{LW}) and the AB components (ΔG_{TOT}^{AB}) of the solid surface and the given biological particle (bacteria, proteins, cells, etc.) in a given medium, is less than zero, that is: $\Delta G_{TOT} = \Delta G_{TOT}^{LW} + \Delta G_{TOT}^{AB} < 0$. In the opposite case, that is, when $\Delta G_{TOT} > 0$, there will be repulsion.

In our lab, we have applied this approach to predict the adhesion of 11 strains of the bacterium *Staphylococcus epidermidis* on 16 TiO_2 nanofilms produced by anodic oxidation.[66] The strains were isolated from infections produced in implants, and their sample free energy was determined elsewhere.[67] For comparison purposes, pyrolytic carbon data were used to predict the adhesion of these strains. The model predicted that 91% of the strains will adhere on pyrolytic carbon and that, in TiO_2 nanofilms, in six cases, none of the strains will adhere, whereas in others, up to 91% of the strains will adhere.[66] These model results will be further compared and validated with experimental results.

Hemocompatibility

Materials that will be in contact with blood must satisfy the standard hemocompatibility criterion of no alteration of the blood equilibrium, should not generate thrombus or damage blood cells, and must not alter the plasma proteins.[8,11,68] In vitro tests to evaluate the degree of hemocompatibility of a material include platelet adhesion and activation, erythrocyte hemolysis, measurement of the clotting time, thrombin time and prothrombin time, and protein adsorption tests.[8,11] Each of these methods gives a measure of the effect of the material on the different steps of the coagulation process.

In our lab, we tested 15 TiO_2 nanofilms produced by anodic oxidation, some of which were subjected to thermal treatment, for platelet adhesion. The films had different roughness, crystalline structure, thickness, and texture. For comparison purposes, we also tested a mirror polished surface of uncoated TiG5 alloy.[69] The results showed that, in nine nanofilms, platelet adhesion was significantly lower than in the uncoated alloy. In the other six nanofilms, adhesion was similar to that found in the TiG5 alloy. These results show the excellent ability of specific TiO_2 coating to reduce adhesion.[69]

The prothrombin time (PT) test allows for the determination of the consumption of factors of the extrinsic pathway of the coagulation chain, whereas the activated partial thromboplastin time (APTT) test determines the consumption of factors of the intrinsic way of the coagulation chain.[10] This technique has been used to indicate whether the presence of different TiO_2 anodic nanofilms alters the normal coagulation process.[11,30] As expected for this material, none of them produced a significant alteration of the coagulation process.[11,30]

CURRENT RESEARCH

The sol–gel and anodic oxidation methods allow obtaining, by parameter adjustments, thin coatings of TiO_2 with smooth or porous surfaces. Porous

surfaces are needed for applications as different as dental and photocatalysis. In the case of dental applications, porous coatings are needed to favor osseointegration,[70–72] whereas in the case of photocatalytic applications, a larger surface area/volume ratio increases the photocatalytic activity in smaller areas of immobilized material, as with porous or nanotubular structures.[73,74] Current research is aimed at introducing chemical substances into TiO_2 coatings and obtain a surface topology with bioactive properties.[75,76] In the case of photocatalysis, doping can narrow the wide band gap of TiO_2 (3.2 eV) to include visible wavelength as active radiations.[77,78]

In the case of permanent implants in humans, like heart valves or other devices in the circulatory system, research is needed to improve wear and corrosion resistance, which have been the main causes of failure of implants.[79] Thus, the current research is also aimed at improving the adherence, mechanical resistance, corrosion resistance, and bio- and hemocompatibility properties of coatings. In the case of orthopedic applications, different techniques, such as functionally grading the coating,[80] laser-induced surface oxidation, roughening,[81] and obtaining surface nano-architectures that may also improve the mechanical and corrosion properties of the coating,[82] are being investigated. Other methods to improve the mechanical properties of the coatings, in particular the wear resistance in the case of the sol–gel coating process, are the sol aging time and the incorporation of reinforcements as SiO_2 particles[83] and postcoating treatments as calcination at different temperatures.[84] The corrosion properties of Ag-doped TiO_2 coatings have been recently investigated in a simulated body fluid solution and other biological environments,[85,86] in an effort to incorporate doping elements that may improve the microbiological properties of the coatings. In the case of bio- and hemocompatibility properties, efforts are being made to investigate other processes to produce superhemophobic titania surfaces[87] as well as micro-arc oxidation coatings. Finally, other uses as biocompatible material have been recently investigated. These include titanium dioxide-coated, gas-exchange membranes for application in bioartificial lungs[88] and the degree of roughness of titanium dioxide to control adhesion, so as to either promote or prevent the adhesion of different cell types,[89] as in the case of the growth of new bone cells to improve osseointegation.[90]

REFERENCES

1. Y. Zhang, Y. Tang, W. Li, and X. Chen, *Chem. Nano Mater.* 1, 1 (2016).
2. M. Kurttepeli, S. Deng, F. Mattelar, D.J. Cott, P. Vereeckens, J. Dendooven, C. Deteavernier, and S. Bals, *ACS Appl. Mater. Interfaces.* 9, 8055 (2017).
3. M.I. Litter, *Advances in Chemical Engineering Photocatalytic Technologies*, ed. H.I. de Lasa and B.S. Rosales (Atlanta: Elsevier, 2009), p. 37.
4. D. Robert, V. Keller, and N. Keller, *Photocatalysis and Water Purification. From Fundamentals to Recent Applications*, ed. P. Pichat (Weinheim: Wiley, 2013), p. 145.
5. L. Rasmusson, J. Roos, and H. Bistedt, *Clin. Implant Dent. Relat. Res.* 7, 36 (2005).
6. A. Besinis, S.D. Hadi, H.R. Le, C. Tredwin, and R.D. Handy, *Nanotoxicology* 11, 327 (2017).
7. E. Bertran-Partida, B. Valdez-Salas, M. Curiel-Alvarez, S. Castillo-Uribe, A. Escamilla, and N. Nedev, *Mater. Sci. Eng., C* 76, 59 (2017).
8. C.E. Schvezov, M.A. Alterach, M.L. Vera, M.R. Rosenberger, and A.E. Ares, *JOM* 62, 84 (2010).
9. N. Huang, P. Yang, Y.X. Leng, J.Y. Chen, H. Sun, J. Wang, P.D. Ding, T.F. Xi, and Y. Leng, *Biomaterials* 24, 2177 (2003).
10. J.Y. Jiang, J.L. Xu, Z.H. Liu, L. Deng, B. Sun, S.D. Liu, L. Wang, and H.Y. Liu, *Appl. Surf. Sci.* 347, 591 (2015).
11. M.L. Vera, J. Schuster, M.R. Rosenberger, H. Bernard, C.E. Schvezov, and A.E. Ares, *Proc. Mater. Sci.* 8, 366 (2015).
12. D. Velten, V. Biehl, F. Aubertin, B. Valeske, W. Possart, and J. Breme, *J. Biomed. Mater. Res. A* 59, 18 (2002).
13. J.X. Liu, D.Z. Yang, F. Shi, and Y.J. Cai, *Thin Solid Films* 429, 225 (2003).
14. C.J. Brinker and A.J. Hurd, *J. Physics III* 4, 1231 (1994).
15. H. Zhang and J. Banfield, *Am. Min.* 84, 528 (1999).
16. P.C. Favilla, M.S. Thesis (UNSaM, CNEA-Instituto de tecnología J. Sabato, Buenos Aires, 2009).
17. M.L. Vera, M.A. Alterach, M.R. Rosenberger, D.G. Lamas, C.E. Schvezov, and A.E. Ares, *Nanomater. Nanotechnol.* 4, 10 (2014).
18. N. Masahashi, Y. Mizukoshi, S. Semboshi, and N. Ohtsu, *Appl. Catal. B* 90, 255 (2009).
19. A.K. Sharma, *Thin Solid Films* 208, 48 (1992).
20. A. Alajdem, *J. Mater. Sci.* 8, 688 (1973).
21. M.V. Diamanti and M.P. Pedeferri, *Corros. Sci.* 49, 939 (2007).
22. T. Shibata and Y.-C. Zhu, *Corros. Sci.* 37, 133 (1995).
23. D. Capek, M.P. Gigandet, M. Masmoudi, M. Wery, and O. Banakh, *Surf. Coat. Technol.* 202, 1379 (2008).
24. T.H. Teh, A. Berkani, S. Mato, P. Skeldon, G.E. Thompson, H. Habazaki, and K. Shimizu, *Corros. Sci.* 45, 2757 (2003).
25. M.L. Vera, A.E. Ares, D. Lamas, and C.E. Schvezov, *An. Asoc. Fis. Argent.* 20, 1850 (2008).
26. H. Habazaki, M. Uozumi, H. Konno, K. Shimizu, P. Skeldon, and G.E. Thompson, *Corros. Sci.* 45, 2063 (2003).
27. Y.T. Sul, C.B. Johansson, S. Petronis, A. Krozer, Y. Jeong, A. Wennerberg, and T. Albrektsson, *Biomaterials* 23, 491 (2002).
28. J.S.L. Leach and B.R. Pearson, *Corros. Sci.* 28, 43 (1988).
29. M.V. Diamanti, F. Bolzoni, M. Ormellese, E.A. Pérez-Rosales, and M.P. Pedeferri, *Corros. Eng., Sci. Technol.* 45, 428 (2010).
30. M.L. Vera, Ph.D. Dissertation (UNSAM. CNEA - Instituto de Tecnología J. Sabato, Buenos Aires, 2013).
31. M.L. Vera, A. Colaccio, M.R. Rosenberger, C.E. Schvezov, and A.E. Ares, *Coatings* 7, 39 (2017).
32. A.I. Kociubczyk, M.L. Vera, C.E. Schvezov, E. Heredia, and A.E. Ares, *Proc. Mater. Sci.* 8, 65 (2015).
33. M.L. Vera, M.R. Rosenberger, C.E. Schvezov, and A.E. Ares, *Int. J. Biomater.* 2015, 9 (2015).
34. M.R. Rosenberger, O.N. Amerio, and C.E. Schvezov, *Mech. Comput.* 24, 1943 (2005).
35. W.L. Lim, Y.T. Chew, H.T. Low, and W.L. Foo, *J. Biomech.* 36, 1269 (2003).
36. T.S. Andersen, P. Johansen, B.O. Christensen, P.K. Paulsen, H. Nygaard, and J.M. Hasenkam, *Ann. Thorac. Surg.* 8, 34 (2006).
37. M.R. Rosenberger, L.A. Guerrero, M.L. Vera, and C.E. Schvezov, *An. Asoc. Fis. Argent.* 24, 71 (2013).
38. M. Boteros, *Caracterización de las propiedades Tribologicas de recubrimentos Duros*, Unviersidad de Barcelona (2005).
39. S. Jacobsson, M. Olsson, P. Hedenqvist, and O. Vingsbo, *ASM Handbook Volume 18: Friction, Lubrications and Wear Technology*, ed. P.J. Blau (Materials Park: ASM International, 1997), pp. 820–837.

40. P. Chalker, S. Bull, and D. Rickerby, *Mater. Sci. Eng., A* 140, 583 (1991).
41. P. Bodo and J.E. Sundgren, *J. Appl. Phys.* 60, 1161 (1986).
42. S. Bull and E. Berasetegui, *Tribol. Int.* 39, 99 (2006).
43. M.L. Vera, M.R. Rosenberger, C. Schvezov, and A. Ares, *Adhesion of Anodic Titanium Dioxide Coatings on Titanium Grades 5 Alloys*, *Symposium: Biological Materials Science Symposium. TMS 2015 Annual Meeting and Exhibition* March 15–19, 2015, Orlando, FL.
44. E. Rabinowicz, *Friction and Wear of Materials*, 2nd ed. (New York: Wiley, 1995).
45. S.C. Lim and M.F. Ashby, *Acta Metall.* 35, 1 (1987).
46. M.A. Alterach, P.C. Favilla, M.R. Rosenberger, D.G. Lamas, A.E. Ares, and C.E. Schvezov, *An. Asoc. Fis. Argent.* 20, 147 (2008).
47. M.L. Vera, M.R. Rosenberger, C.E. Schvezov, and A.E. Ares, *Nanomater. Nanotechnol.* 5, 1 (2015).
48. J.M. Schuster, M.R. Rosenberger, and C.E. Schvezov, *Wear of TiO_2 Nanofilms Synthetized on Ti6Al4 V and 316 Stainles Steel*, *TMS 2017, 146th Annual Meeting and Exhibition*, San Diego, CA.
49. X. Liu, P.K. Chu, and C. Ding, *Mater. Sci. Eng.* 49, 49 (2004).
50. C. Leyens and M. Peters, *Titanium and Titanium Alloys; Fundamentals and Applications*, 1st ed. (Cologne: Wiley, 2003), p. 512.
51. H. Reza, A. Bidhendi, and M. Pouranvari, *Metall. Mater. Eng.* 17, 13 (2011).
52. S. Kumar, T.S.N. Sankara Narayanan, S. Ganesh Sundara Raman, and S.K. Seshadri, *Corros. Sci.* 52, 711 (2010).
53. S.A. Fadl-allah and Q. Mohsen, *Appl. Surf. Sci.* 256, 5849 (2010).
54. S. Tamilselvi, V. Raman, and N. Rajendran, *Electrochim. Acta* 52, 839 (2006).
55. M. Schaldach, *Electroterapia del Corazón, Aspectos técnicos en Estimulación Cardiaca* (New York: Springer, 1993), p. 253.
56. M. Atapour, A.L. Pilchak, G.S. Frankel, and J.C. Williams, *Mater. Sci. Eng., C* 31, 885 (2011).
57. J.R. Galvele and G.S. Duffó, *Desgradación de Materiales: Corrosión*, 1st ed. (Buenos Aires, Jorge Bauino Ediciones: Instituto Sabato, 2006).
58. M.L. Vera, E. Linardi, L. Lanzani, C. Mendez, C.E. Schvezov, and A.E. Ares, *Mater. Corros.* 66, 1140 (2015).
59. C.J. Van Oss, *Interfacial Forces in Aqueous Media*, 2nd ed. (Boca Raton, FL: CRC Press, 2006).
60. C.L. Perini, Q. Zhao, Y. Liu, and E. Abel, *Colloids Surf. B* 48, 143 (2006).
61. J.M. Schuster, C.E. Schvezov, and M.R. Rosenberger, *Proc. Mater. Sci.* 8, 742 (2015).
62. M. Żenkiewicz, *J. Achiev. Mater. Manuf. Eng.* 24, 137 (2007).
63. J.M. Schuster, C.E. Schvezov, and M.R. Rosenberger, *Proc. Mater. Sci.* 8, 732 (2015).
64. J.M. Schuster, M.L. Vera, C.E. Schvezov, and M.R. Rosenberger, *Hidrofobicidad y Tensión Superficial de Nanopelículas de Dióxido de Titanio*. 100ª (Reunión Nacional de la Asociación Física Argentina 2015). San Luis.
65. C.J. Van Oss, *The Properties of Water and Their Role in Colloidal and Biological Systems*, 1st ed., vol. 16 (Waltham, MA: Academic Press, 2008).
66. J.M. Schuster, M.L. Vera, C.E. Schvezov, and M.R. Rosenberger, *Estudio de la Adhesión Microbiana de Staphylococcus Epidermidis en Nanopelículas de TiO_2: Predicción Teórica*. 100ª (Reunión Nacional de la Asociación Física Argentina San Luis, Argentina, 2015).
67. C. Sousa, P. Teixeira, and R. Oliveira, *Int. J. Biomater.* 1 (2009).
68. K.C. Dee, D.A. Puleo, and R. Bizios, *An Introduction to Tissue-Biomaterial Interactions*, 1st ed. (New York: Wiley, 2002).
69. J.M. Schuster, M.L. Vera, M.E. Laczeski, M.R. Rosenberger, and C.E. Schvezov, *TMS 2015 Supplemental Proceedings* (Warrendale, PA: TMS, 2015), pp. 653–660.
70. R. Thull, *Biomol. Eng.* 19, 43 (2002).
71. J.E. Ellingsen, *Periodontol* 2000, 36 (1998).
72. C.N. Elias, Y. Oshida, J.H. Cavalcanti Lima, and C.A. Muller, *J. Mech. Behav. Biomed. Mater.* 1, 234 (2008).
73. H.D. Traid, M.L. Vera, A.E. Ares, and M.I. Litter, *Mater. Chem. Phys.* 191, 106 (2017).
74. D. Regonini, C.R. Bowen, A. Jaroenworaluck, and R. Stevens, *Mater. Sci. Eng., R* 74, 377 (2013).
75. A.L. Oliveira, J.F. Mano, and R.L. Reis, *Curr. Opin. Solid State Mater. Sci.* 7, 309 (2003).
76. F. Barrere, M.M.E. Snel, C.A. van Blitterswijk, K. de Groot, and P. Layrolle, *Biomaterials* 25, 2901 (2004).
77. M. Pelaez, N.T. Nolan, S.C. Pillai, M.K. Seery, P. Falaras, A.G. Kontos, P.S.M. Dunlop, J.W.J. Hamilton, J.A. Byrne, K. O'Shea, M.H. Entezari, and D.D. Dionysiou, *Appl. Catal. B* 125, 331 (2012).
78. L. Sun, J. Li, C.L. Wang, S.F. Li, H.B. Chen, and C.J. Lin, *Sol. Energy Mater. Sol. Cells* 93, 1875 (2009).
79. D. Scharnweber, *Metals as Biomaterials*, ed. J.A. Helsen and H.J. Breme (New York: Wiley, 1998),.
80. A. Sola, B. Devis, and V. Cannillo, *Biotechnol. Adv.* 34, 504 (2016).
81. S. Zimmermann, U. Specht, L. Spie, H. Romanus, S. Krischok, M. Himmerlich, and J. Ihde, *Mater. Sci. Eng., A* 558, 755 (2012).
82. S. Wu, X. Liu, K.W.K. Yeung, H. Guo, P. Li, T. Hu, C. Yuen Chung, and P.K. Chu, *Surf. Coat. Technol.* 233, 13 (2013).
83. M. Yazıcı, O. Çomaklı, T. Yetim, A.F. Yetim, and A. Celik, *Tribol. Int.* 104, 175 (2016).
84. O. Çomaklı, T. Yetim, and A. Çelik, *Surf. Coat. Technol.* 246, 34 (2014).
85. T. Yetim, *J. Bionic Eng.* 13, 397 (2016).
86. T. Yetim, *Surf. Coat. Technol.* 309, 790 (2017).
87. S. Movafaghi, V. Leszczak, W. Wang, J.A. Sorkin, L.P. Dasi, K.C. Popat, and A.K. Kota, *Adv. Healthc. Mater.* 6, 4 (2017).
88. M. Pflaum, M. Kuehn-Kauffeldt, S. Schmeckebier, D. Dipresa, K. Chauhan, B. Wiegmann, R.J. Haug, J. Schein, A. Haverich, and S. Korossis, *Acta Biomater.* 50, 510 (2017).
89. M. Kulkarni, A. Mazare, E. Gongadze, Š. Perutkova, V. Kralj-Iglič, I. Milošev, and M. Mozetič, *Nanotechnology* 26, 062002 (2015).
90. M. Vandrovcova, J. Hanus, M. Drabik, O. Kylian, H. Biederman, V. Lisa, and L. Bacakova, *J. Biomed. Mater. Res. A* 100, 1016 (2012).